Techno-Economic Planning and Exergy Analysis of Large-Scale Hot-Water Tank and Pits

Abdulrahman Dahash
Sustainable Thermal Energy Systems
Center for Energy, AIT Austrian Institute of Technology GmbH
Vienna, Austria
Abdulrahman.Dahash@ait.ac.at

Fabian Ochs
Unit of Energy Efficient Buildings
University of Innsbruck
Innsbruck, Austria
Fabian.Ochs@uibk.ac.at

Alice Tosatto
Unit of Energy Efficient Buildings
University of Innsbruck
Innsbruck, Austria
Alice.Tosatto@uibk.ac.at

***Abstract* — Large-scale seasonal thermal energy storage (STES) substantially facilitates a full exploitation of the local renewable energy sources (e.g. geothermal, solar, waste heat) potential in renewables-based district heating systems in order to mitigate CO_2 emissions and the climate change. Large-scale seasonal TES systems store energy for lengthy timescales; therefore, it is essential to properly plan these structures in order to avoid high capital cost and/or performance below expectations.**

The STES planning phase includes a wide list of variables such as hydrogeological conditions (e.g. soil type, groundwater existence and/or flowing), TES geometry (e.g. tanks, conical pits, pyramid stump pits), TES construction (e.g. freestanding, partially or fully buried), system characteristics (e.g. operation temperatures), liners and insulation and others. Therefore, it is crucial to strive for an optimal TES selection in which a compromise between the technical performance and the economic investment is made.

This work examines the planning of large-scale TES systems by means of numerical simulations. The models used are calibrated using measured data from the pit thermal energy storage in Dronninglund (Denmark). For the techno-economic assessment, different key performance indicators are used such as: energetic efficiency, exergetic efficiency, stratification efficiency and levelized cost of stored heat (LCOS). In this context, the investigation depicts that a hybrid TES arises as a promising option that combines the advantages of both tank and shallow pit. Accordingly, hybrid LCOS deems to be the lowest among other geometries. Further, the examination reveals that a tank has better technical performance and lower LCOS than a shallow pit under the same set of boundary conditions.

Considering the transition to low-temperature district heating (DH) systems, the work further investigates the influence of DH temperature on TES techno-economic performance. Not only does the low-temperature DH lead to an increase in TES performance but it also results in lower LCOS compared to its counterpart in a DH with high-temperature.

Keywords* — *Large-scale thermal energy storage; Renewable district heating; Techno-economic analysis; Levelized cost of stored heat; Planning and construction; Exergy analysis.

I. INTRODUCTION

The establishment of renewables-based district heating systems is emphasized by the utilization of the locally available renewable resources that can be integrated into district boundaries and used to satisfy the heat demand. Such resources include geothermal energy, solar energy or wind energy that requires the installation of power-to-heat technologies. Besides, waste heat can be also integrated; thus, it also emerges as a key heat resource [1].

Despite the significance of such resources, there exist some challenges and frontiers hindering the utilization and the robust reliance on renewables. Among others, a major issue is the peak load of the buildings stock. Thus, the availability of renewables might mismatch with peak load. Therefore, peak shaving becomes crucial in order to supply the DH end-users with affordable efficient heat [2].

Another challenge is the seasonal mismatch between the available resources and the buildings' heat demand. The availability of renewable resources (i.e. solar energy, wind energy) depends on site location and time-horizon, whereas the accessibility to these resources relies on the technologies used. As the site location aspect holds true for geothermal energy and waste heat, it is important to pay attention that geothermal heat can be generated at nearly constant rate. Whilst waste heat can have a constant or volatile

pattern. In contrast, the buildings' heat demand is strongly linked to the outdoor temperature (besides occupancy, users' behavior and building envelope); thus, the resulting heat demand varies seasonally and daily [3]. This leads to a difference between the heat demand and heat supply. Consequently, this mismatch might reduce the use of renewables and excess heat [4].

A key player to bridge the seasonal gap is the large-scale thermal energy storage (TES). Herein, the common types are: 1) aquifer TES (ATES), 2) borehole TES (BTES), 3) tank TES (TTES) and 4) pit TES (PTES). Both ATES and BTES will not be further considered as they are capable to operate with moderate flowrates, whereas the work focuses on TTES and PTES as they achieve high charging/discharging flowrates favorable for DH systems [5].

Earlier studies demonstrated that the design, planning and construction of large-scale TES is often anticipated as a complex process. For instance, Dahash et al. [6] emphasized the role played by different variables (e.g. location, TES size, TES geometry, hydrogeological conditions and others) on the planning of tanks and pits. Therein, the work concluded that the planning of such technologies is an interconnected process whereby every individual variable might alter the entire planning as demonstrated in Fig. 1**.** Therefore, simulation-driven planning emerges as a key solution to quantify the influence of several boundary conditions on TTES and PTES planning. Thus, calibrated numerical TES models are of great importance as they are the viable means for such investigations [7].

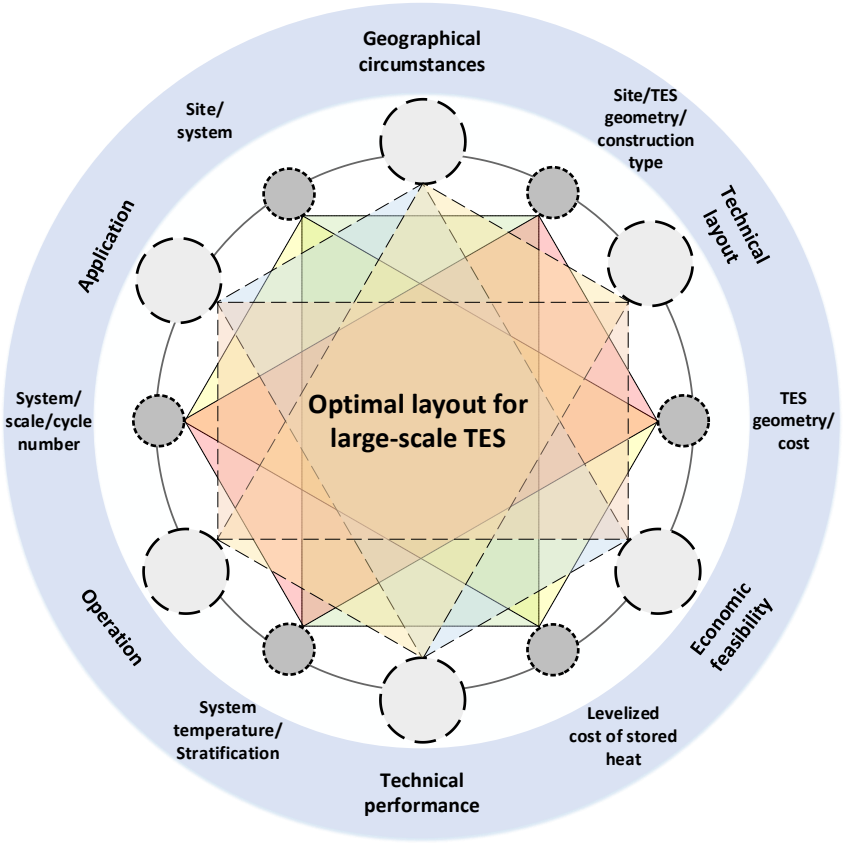

Fig. 1: Presentation of the most influencing parameters on the construction of large-scale underground TES and its economic feasibility.

II. LITERATURE REVIEW

The planning and construction phases of TES have been at the spot in an increasing number of research and development activities. This awareness is strongly ascribed to the fact that large-scale TES systems demand a space availability due to the substantial great volume required to efficiently accomplish the long-term tasks (i.e. storage periods) [8]. Therefore, it is important to address all the relevant questions during the planning phase when seeking the optimal TES for a specific R-DH system. Otherwise, the capital investment cost might be lost when the TES performance is below expectations and the goal (e.g. abatement of CO_2 and reduction of fossils) is not achieved. Such questions usually concern a group of players that might have an impact of TES techno-economic performance. These questions include hydrogeological conditions (e.g. soil type, groundwater existence and/or flowing), TES geometry (e.g. tanks, conical pits, pyramid stump pits), TES construction (e.g. freestanding, partially or fully buried), system characteristics (e.g. operation temperatures), liners and insulation and others. In this context, large-scale TES

planning and construction dependency on these questions and others is revealed in [8]. It is found that addressing answers to these questions play a critical role in the techno-economic assessment of such stores. Hence, it is crucial to strive for an optimal TES selection in which a compromise between the technical performance and the economic investment is made.

In this context, Ochs et al. [1] examined a number of design parameters of the large-scale TES on the investment cost in a techno-economic analysis framework. Therein, the TES volumes considered are typically between 100,000 m^3 and 2,000,000 m^3 for two main types of STES: 1) tank TES and 2) pit TES. On their part, the authors highlight the role of TES cover as the work observed cheaper specific costs for the configurations of PTES that are equipped with floating covers compared to their counterparts. Yet, the work highlighted the infeasibility of PTES configurations equipped with trafficable covers compared to the tank and, thus, tank TES arise as feasible option.

Seeking for sustainability assessment of R-DH system, the optimal integration of solar-assisted district heating system (S-DH) for different urban sized communities was investigated in [9]. The work paid attention to the multi-objective optimization of such systems. Besides, it paid noteworthy efforts towards developing a robust machine learning model to tackle the computational challenges associated in optimization problems for TRNSYS models. The aim of the work was the inspection of techno-economic-environmental feasibility for S-DH. The work considered a partially buried seasonal TES with a circular cross-section and a geometry shown in Fig. 2(c). Yet, the work did not thoroughly investigate the techno-economic planning of the TES considering different construction types and geometries.

Panthalookaran et al. [10], on their part, conducted a technical analysis with the aid of numerical simulations via development of numerical CFD models. The work brought the impact of TES geometrical parameters to the light paying considerable awareness to thermal stratification. Such parameters were: the TES geometry, TES internal structure, TES volume (2,500 m^3 – 12,000 m^3) and aspect ratio between 0.5 and 3. The TES geometries considered in the work are shown in Fig. 2. Amongst others, the TES options with slopped walls in the bottom arise as the efficient ones.

On their part, Yang et al. [11] conducted a thermo-economic analysis for a solar-assisted district heating with a seasonal thermal energy storage using dynamic simulations via TRNSYS. The work found that increasing the solar fraction led to a decrease in the heating price. Yet, the depreciation and loan played a critical role in the determination of the heating price.

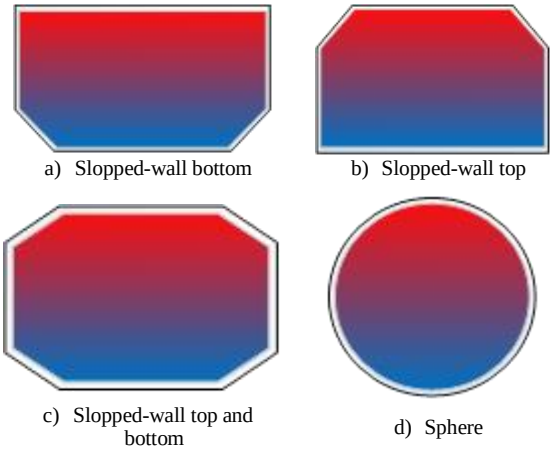

Fig. 2: Possible TES geometries for large-scale applications

Moreover, literature investigated the exploitation of underground rock caverns as hot-water TES due to their large volume. However, such stores are naturally formed, and they are not manmade and, therefore, it is important to examine their suitability for storing thermal energy. As a result, Park et al. [12] conducted a numerical investigation to understand the thermal behavior in such stores. Thus, the work considered a case study that was Lyckebo rock cavern in Sweden. The cavern has a volume of 100,000 m^3. The outcomes clearly addressed the impact of cavern aspect ratio and surrounding rocks temperature on the stratification quality.

In the aforementioned literature, the examination mostly considered indicators that are based on the 1st of thermodynamics. Despite their suitability, such measures might be incapable to capture the entire planning picture when a large-scale seasonal TES is envisioned in the considered system [8]. This incapability is attributed to the wide list of parameters that have to be repeatedly examined in the planning framework. Besides, it is crucial to underline the absence of a comprehensive energy efficiency measure that is capable to capture also the internal thermal losses in TES.

A. Contribution of this work

In this study, the authors demonstrate the influence of TES geometry on thermal stratification for a given R-DH by conducting a technical analysis for two geometries (cylindrical TES and cone PTES) as presented in Fig. 3 (a) and (b). In this context, numerous performance indicators are introduced in order to carry out the analysis. As a result, the work proposes a third TES geometry illustrated in Fig. 3 (c), which combines both TTES and PTES configuration in order to obtain the benefits of both geometries.

Thee examined TES geometries in this work are presented in Fig. 3. The dimensions and characteristics are reported in TABLE I, TABLE II and TABLE III for the types tank, shallow pit and hybrid, respectively. In this regard, an earlier work [13] considered a

groundwater flow in the TES surroundings and, subsequently, the work attempted to pave a framework for techno-economic-environmental guidelines for TES installation with groundwater. As a result, this current work sets the path for detailed techno-economic guidelines that can be used for planning under favorable hydro-geological conditions (i.e. no groundwater existence or flowing) and for a given set of boundary conditions for R-DH.

Moreover, it is essential to design STES systems with favorable aspect ratios and proper geometries. Thus, exergy efficiency arises as a good indicator since it is capable to emphasize the influence of mixing losses that are basically temperature losses affecting the quality of discharged amount of heat. Thus, this work will utilize different performance measures (i.e. energy efficiency, exergy efficiency) and stratification quality measures (e.g. stratification efficiency, *Str(t)*) when seeking the optimal STES.

Furthermore, the work extends the investigation to a techno-economic analysis framework. Thus, the work reports the levelized cost of stored heat (LCOS) for each TES geometry and volume investigated. The importance of this indicator (i.e. LCOS) is that it crucially pinpoints the role of TES geometry and volume on the technical performance and the stored heat unit price. As a result, the main goal of this work is the pavement and concrete establishment of detailed guidelines for techno-economic analysis of large-scale seasonal thermal energy storage. This work can be later a great aid to engineers and researchers in this field to plan efficient and effective large-scale TES. Such a detailed framework will lead to a reduction in the planning time and an easy navigation through the optimal TES solution for the considered DH system.

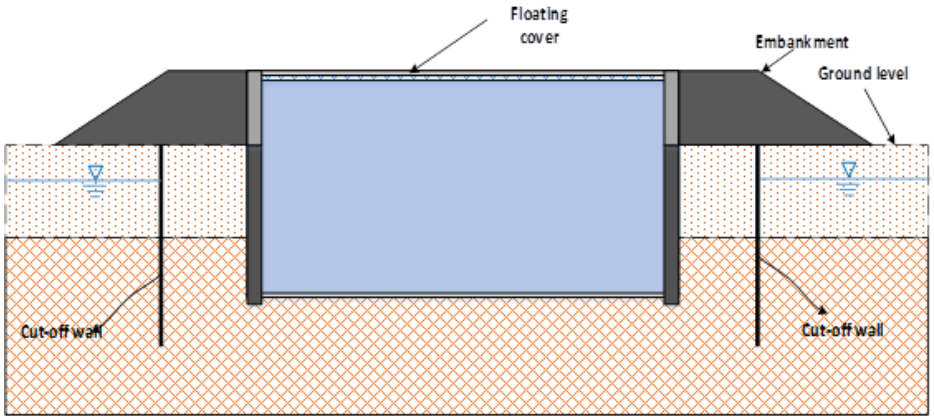

a) Tank

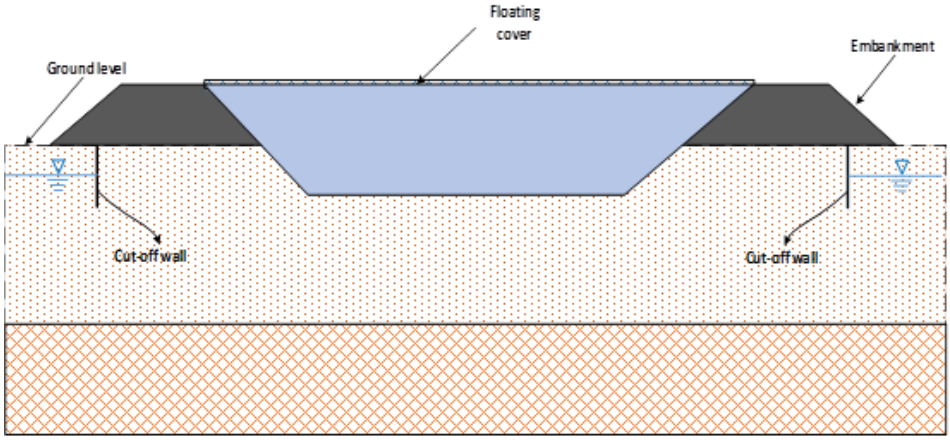

b) Shallow pit

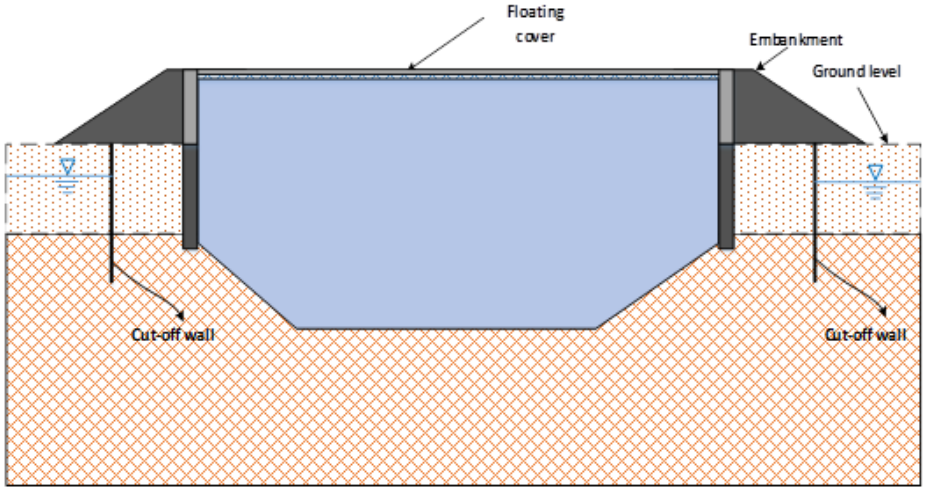

c) Hybrid – combination of tank and shallow pit

Fig. 3: Different TES geometries considered in this work.

TABLE I. TANK TES DIMENSIONS.

	Case 1	Case 2	Case 3
Height, H [m]	50	50	50
Diameter, d [m]	50.46	112.83	225.67
Surface area, SA [m^2]	11927	37725	115449
Volume, V [m^3]	100,000	500,000	2,000,000
H/d [-]	0.991	0.443	0.222
SA/V [1/m]	0.119	0.075	0.058
Slope, α [°]	90	90	90

TABLE II. SHALLOW PIT TES DIMENSIONS[1].

	Case 1	Case 2	Case 3
Height, H [m]	10.5	13.8	17.7
Top diameter, d_{top} [m]	127.8	238.3	409.5
Bottom diameter, d_{bot} [m]	91.4	190.5	348.1
Surface area, SA [m^2]	26620	91669	268997
Volume, V [m^3]	100,000	500,000	2,000,000
H/d [-]	0.096	0.064	0.047
SA/V [1/m]	0.266	0.183	0.134
Slope, α [°]	30	30	30

TABLE III. HYBRID TES DIMENSIONS.

	Case 1	Case 2	Case 3
Height, H_{pit} [m]	10	7	12
Height, H_{tank} [m]	11.94	15	30.24
Height, H [m]	21.94	22	42.24
Top diameter, d_{top} [m]	88.25	174.45	252
Bottom diameter, d_{bot} [m]	62.36	146	204
Surface area, SA [m^2]	14063	56842	125723
Volume, V [m^3]	100,000	500,000	2,000,000
H/d [-]	0.31	0.14	0.19
SA/V [1/m]	0.14	0.11	0.06
Slope, α [°]	48	26	26

III. METHODOLOGY

In principle, the TES models are developed relying on the axisymmetric representation for TES geometries with circular cross-section. Fig. 4 schematically shows the TES system in interaction with the surrounding ground. Therein, it is seen that the TES is equipped with multiport for charging/discharging processes. Thus, the storage medium domain inside the TES is capable to emulate several TES ports (i.e. multiport model) and this permits the user to allocate the charging/discharging ports at the desired height. Besides, it is possible to discretize the TES into n segments. Herein, it is important to mention that TES segments are divided with equal volumes instead of equal distances (i.e. equidistant heights) in order to maintain a segmental energy balance for sloped-wall TES. For each segment (i), the constraints are energy balance and mass conservation. The segmental energy balance is developed as a partial differential equation and obeys the following:

$$\left(\rho A_i c_p\right)\frac{\partial T_i(t)}{\partial t} = -\left(\rho \dot{V}_{\mathrm{w}} c_p\right)\frac{\partial T_i(t)}{\partial z_i} + A_i \frac{\partial}{\partial z_i}\cdot\left(\lambda_{\mathrm{w,eff}}\frac{\partial T_i}{\partial z}\right) - \dot{q}_{\mathrm{loss},i} \quad (1)$$

$$\dot{q}_{\mathrm{loss},i} = U_{\mathrm{side}} \cdot P_i \cdot \left(T_i(t) - T_{\mathrm{g},i}(t)\right) \quad (2)$$

Where ρ, c_p and λ_{w} represent the density, specific heat capacity and thermal conductivity of the storage medium, respectively. Whereas A_i is the cross-section area of the segment (i). Equation (2) expresses the thermal losses from the corresponding segment (i) to the surroundings and, therein, U_{side} stands for the

[1] The authors chose these dimensions for the shallow pit configuration by purpose in order to highlight the influence of (H/d) and (SA/V) ratio on the TES energetic and exergetic efficiency (i.e. stratification).

overall heat transfer coefficient (HTC) of the TES envelope (fluid to ground). Whilst (P_i) is the segment perimeter.

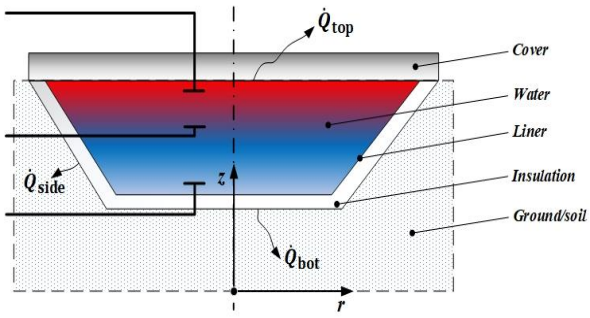

Fig. 4: An exemplary 2-D representation of an underground shallow pit with the different required domains and surroundings [14].

For further information on the model development, the reader is referred to the following literature: [6] and [13]. Therein, the development of the numerical models together with the approach used are addressed in detail. Besides, the works pinpoints the validation of the developed model as this step represents a key stone for the utilization of such model for planning purposes.

A. *Operation scenario, boundary conditions and assumptions*

In this research, the focus is to develop STES models that are reliable and computationally fast enough to give insights on the design of STES. Therefore, system simulations are not considered at this stage and this means no DH system is actually modeled. However, the DH operation profiles (temperature and flowrate) are of importance for the operation of STES system, especially for the charging/discharging modes. Therefore, a simplified standard DH temperature profile is introduced in the model, where the DH supply temperature is set to 90°C and the return temperature is given as 60°C. Fig. 5 and Fig. 6 show the simplified periodic operating conditions for a TES. TABLE IV reports the thermo-physical properties and other significant parameters used for the simulations.

TABLE IV. THERMO-PHYSICAL PROPERTIES OF THE MATERIALS AND HEAT TRANSFER COEFFICIENTS (HTC) OF THE DIFFERENT COMPONENTS IN TES

Parameter	Value
Water thermal conductivity, λ_w	0.6 W/(m.K)
Water density, ρ	1000 kg/m^3
Water specific heat capacity, c_p	4200 J/(kg.K)
Overall HTC of the top (cover), U_{top}	0.1 W/(m^2.K)
Overall HTC of the sidewalls, U_{side}	0.3 W/(m^2.K)
Overall HTC of the bottom, U_{bot}	0.3 W/(m^2.K)
Ground thermal conductivity, λ_g	1.5 W/(m.K)
Ground specific heat capacity, $c_{p,g}$	880 J/(kg.K)
Ground density, ρ_g	1000 kg/m^3

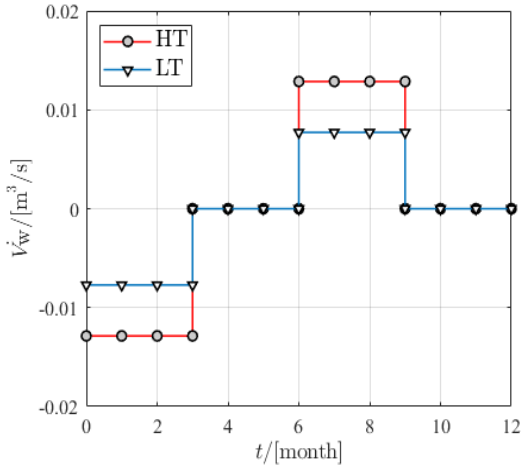

Fig. 5: A year-round incoming/outgoing flowrate for a TES with a volume of 100,000 m^3.

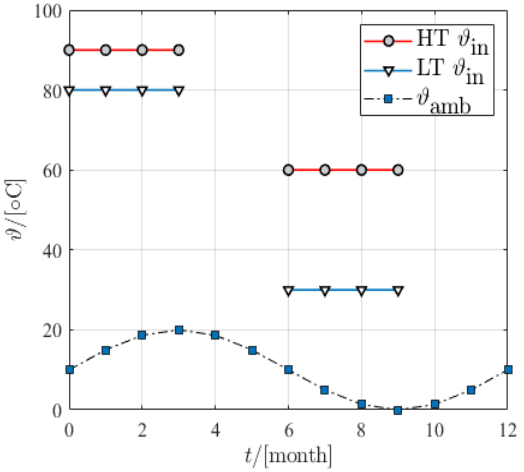

Fig. 6: A year-round injection temperature into TES and ambient temperature as a sinus function with an average of 10°C.

B. *Key performance indicators*

To conduct a thorough performance analysis, it is important to define expressive physics-based quantities that are capable to evaluate the energy performance of one TES and compare it to another in order to support the decision-making process. In this context, numerous indicators (e.g. TES energy efficiency, TES stratification, thermocline thickness) can be found in literature. As a result, this work utilizes 5 metrics for the technical evaluation of the TES. These metrics are divided into metrics that are based on the 1st law of thermodynamics and others based on the 2nd law of thermodynamics.

For the techno-economic analysis, the levelized cost of stored heat (LCOS) emerges as a key measure as it measures the average net present cost of stored heat across the lifecycle of the TES system under consideration. This indicator only accounts for the annualized investment cost (CAPEX) and the operation

and maintenance cost (OPEX) that is 10 % of the CAPEX. LCOS does not account for additional cost for the TES decommissioning after the planned service lifetime. In this context, the service lifetime and the interest rate are 50 years and 3 %, respectively. Furthermore, the denominator ($\sum_{i=0}^{t} Q_{\mathrm{dis}}(t) \cdot \mathrm{d}t$) expresses the total amount of discharged heat for the examined year.

TABLE V reports the key performance indicators used in this work together with their corresponding the description. The reader is referred to [15] if further information on the key performance indicators is needed.

TABLE V. LIST OF THE KEY PERFORMANCE INDICATORS USED IN THE TECHNO-ECONOMIC ANALYSIS (ADAPTED FROM [15]).

KPI	Equation	Description
Energy efficiency	$\eta_{\mathrm{I}} = \frac{Q_{\mathrm{dis}}}{Q_{\mathrm{ch}}}$	Ratio of the heat discharged at useful temperature to the amount of heat charged into the TES.
Energy capacity efficiency	$\eta_{\mathrm{II}} = 1 - \frac{Q_{\mathrm{loss}}}{Q_{\mathrm{TES}}}$	Ratio of the effective storage capacity to the maximum nominal capacity.
Exergy efficiency	$\psi = \frac{EX_{\mathrm{dis}}}{EX_{\mathrm{ch}}}$	Ratio of the exergy discharged to the amount of exergy charged into the TES.
Stratification number	$Str(t) = \frac{\overline{(\partial T/\partial z)}_{\mathrm{t}}}{(\overline{\partial T/\partial z})_{\mathrm{max}}}$	Ratio of the mean temperature gradients at any time to the maximum mean temperature gradient for the discharging/charging process.
Stratification efficiency	$\eta_{\mathrm{Str}} = 1 - \frac{M_{\mathrm{E}}^{\mathrm{stratified}} - M_{\mathrm{E}}^{\mathrm{exp}}}{M_{\mathrm{E}}^{\mathrm{stratified}} - M_{\mathrm{E}}^{\mathrm{fully-mi}}}$	This metric evaluates the TES stratification quality considering each segment temperature and energy content.
Levelized cost of stored heat (LCOS)	$\mathrm{LCOS} = \frac{(C_{\mathrm{inv}} \cdot ANF) + C_{\mathrm{O\&M}}}{\sum_{i=0}^{\tau} Q_{\mathrm{dis}}(t) \cdot \mathrm{d}t}$	Quotient of the annualized storage cost to the discharged heat from the storage.

TABLE VI reports the plant construction and site facilities as fixed costs, and they are independent of the TES volume. However, it must be pinpointed that the values reported in TABLE VI are rough costs estimation based on experience, previous projects and literature.

Furthermore, Dahash et al. [15] highlighted that the installation of a 100,000 m^3 pit with steep edges might lead to improved cost effectiveness and, subsequently, feasibility improvement in terms of economic considerations. In this context, the height of the pit TES can be 16.3 m instead of 10.5 m as illustrated in [1]. However, this work focuses on the impact of TES dimensions on the energetic and exergetic TES efficiency as well as the LCOS. Accordingly, this work chose the dimensions of the shallow pit reported in TABLE II to highlight this impact.

TABLE VI. BREAKDOWN OF THE SPECIFIC COSTS FOR THE CONSTRUCTION OF SEASONAL TES (REPRODUCED FROM [1] AND [16])

Contribution	(Specific) Costs	Remark
Excavation	20 €/m³	Partly wet excavation
Diaphragm wall	550 €/m²	50 m deep, cost without anchors
Cut-off wall	50 €/m²	In case of groundwater in 5 m distance
Sidewall	375 €/m³ 100 €/m²	Insulation cost Insulation installation
Bottom	100 €/m³	Insulation cost and installation (pressure resistant)
Liner	150 €/m² 50 €/m²	VA, Stainless steel (HT) Polymer liner (LT)
Cover	200 €/m² 800 €/m²	Floating cover (50 cm ins.) Trafficable floating cover
Plant construction	40,000 €	Independent TES construction
Site facilities	50,000 €	Fixed

In the previous table, the TES height does not play a major role in the excavation cost. Instead, it is volume dependent. Besides, planning experience has pinpointed the importance of anchors for the construction of tanks with volumes > 200,000 m^3. Thus, it is important to mention that the diaphragm wall cost does not cover the anchors cost. Moreover, this work does not consider groundwater flow nearby the TES surroundings and, subsequently, the cost of the cut-off wall can be excluded. Further, the insulation installation in the sidewalls is more challenging than that in the TES bottom and, accordingly, the sidewall insulation encompasses two components; one is insulation volume dependent, while the other is dependent on the TES lateral area.

IV. TECHNO-ECONOMIC ANALYSIS

A. *Specific investment cost*

To compare the specific investment cost, this work generally considers two TES volumes: 100,000 m^3 and 2,000,000 m^3 as the lower and upper bounds, respectively. The comparison is also expanded to a single option with no insulation and two other cases with insulation thickness (i.e. 12 cm and 26 cm). Further, the comparison encompasses three TES geometries: tank, shallow pit and hybrid.

In this context, Fig. 7 compares the total specific investment cost for the aforementioned options with a volume of 100,000 m^3. Therein, the special geotechnical works can be observed as the most expensive item for the tank case. This is certainly due to the installation of costly diaphragm walls in order to provide stability. Whereas this item is not needed for the shallow pit. However, the shallow pits are often built with poor aspect ratios and, thus, such TES has large top areas compared to their counterparts. Subsequently, the major cost item is attributed to the lid (i.e. TES cover).

The hybrid TES option, on the other hand, arises with notable contribution of both items (i.e. special geotechnical works and cover) in the specific investment cost. However, this TES type is characterized with a major item from the wall insulation compared to its counterparts. Fig. 7 highlights the prominence of the hybrid TES given its economic considerations for the investigated volume.

As for the TES volume of 2,000,000 m^3, Fig. 8 compares the different TES cases and the findings highlights the role of economy-of-scale as the specific investment costs significantly drops compared to its counterparts with a 100,000 m^3. Remarkably, Fig. 8 shows the tank as a cheaper option compared to the shallow pit with 2,000,000 m^3. The reason behind is the expansion of the shallow pit to larger volumes and, subsequently, the increase in the surface area. Thus, a rise in the costs of the cover, wall insulation and bottom insulation compared to its counterparts. Furthermore, Fig. 8 confirms the importance of hybrid TES as a promising option as it has the cheapest specific investment cost among the investigated TES options.

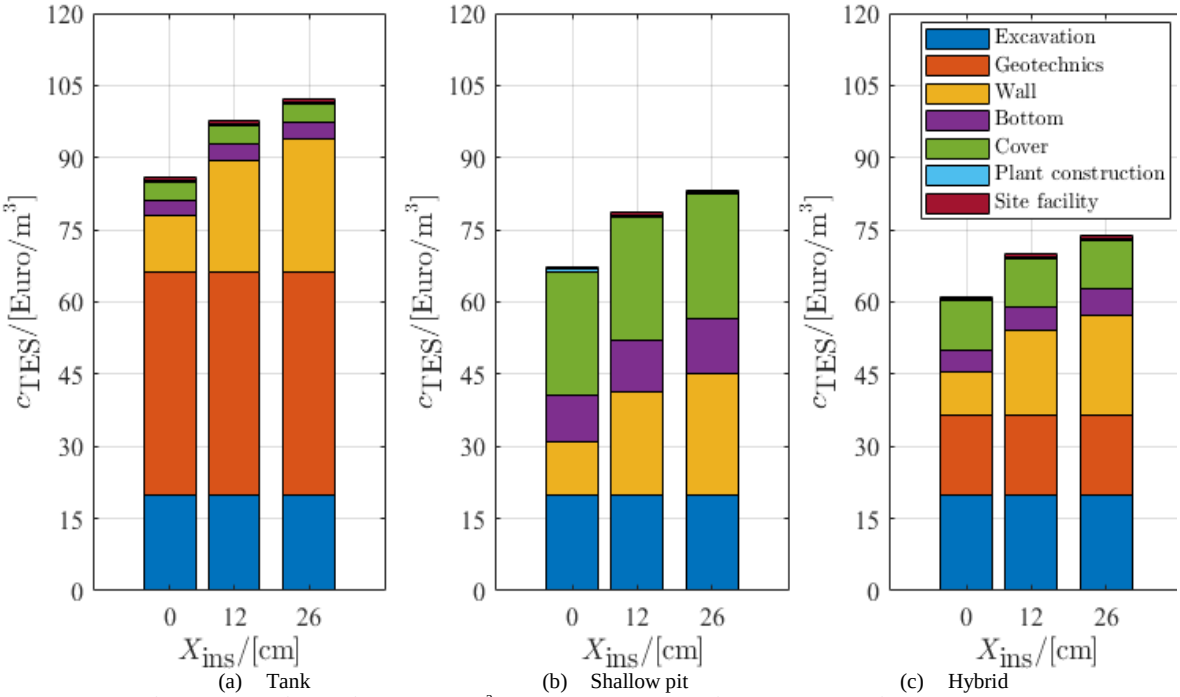

(a) Tank (b) Shallow pit (c) Hybrid

Fig. 7: Breakdown of the total specific cost for a 100,000 m^3 TES installed in HT-DH following the specific component costs in TABLE V.

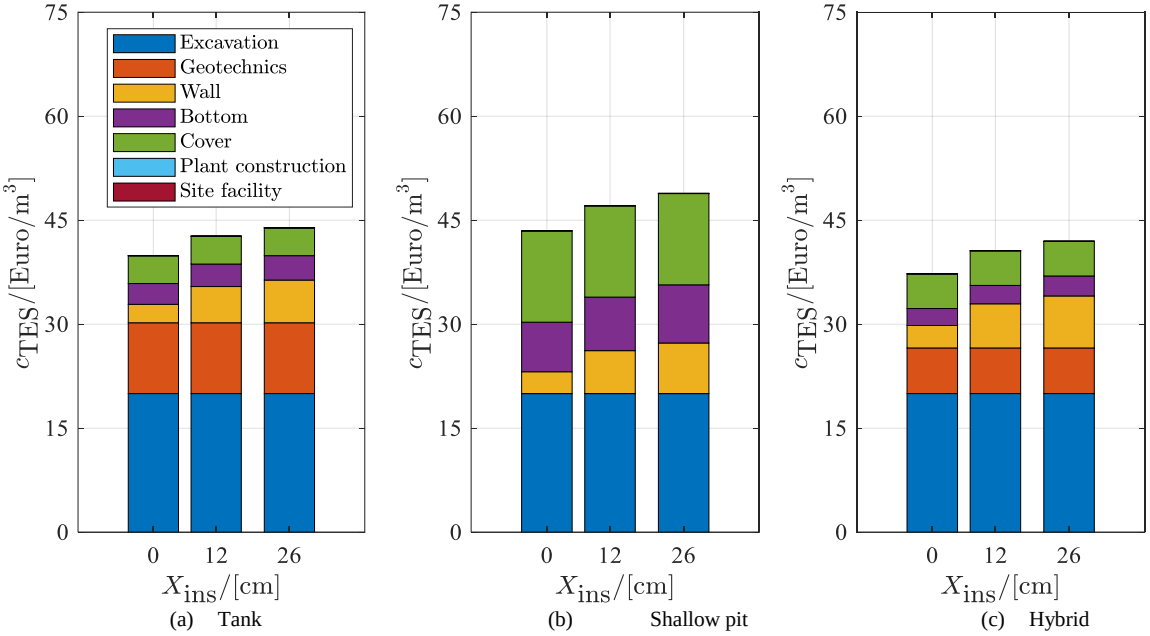

(a) Tank (b) Shallow pit (c) Hybrid

Fig. 8: Breakdown of the total specific cost for a 2,000,000 m^3 TES installed in HT-DH following the specific component costs in TABLE V.

B. Impact of TES geometry

Fig. 9 compares the TES energy efficiency and TES energy capacity efficiency between three geometries (i.e. tank, conical shallow pit and hybrid) for three volumes over different insulation thicknesses. There, it is undoubtedly seen that the tank outperforms the other options. Besides, the tank efficiency surpasses the shallow pit efficiency with a notable amount. On a brighter note, the hybrid TES arises as a promising solution as it comprises both TES options with efficiency approximating the one from the tank. Moreover, Fig. 9 reveals that increasing TES volume does not only bring economic advantages (i.e. economy of scale) but it also helps improve the TES efficiency as TES volume increases. Fig. 10 confirms the findings shown in Fig. 9 as it reveals that the tank owns the highest exergy efficiency, whereas the hybrid arises as a feasible approximation. Further, Fig. 10 affirms the importance of increasing TES volume as it shows that increasing TES volume results in better exergy efficiency.

Fig. 11 reports the levelized cost of stored heat for the TES types considered (i.e. tank, conical shallow pit and hybrid). In this regard, the results highlight the shallow pit TES as the infeasible option due to its highest LCOS compared to the tank. This is attributed to the drop in performance exhibited by the shallow pit in terms of discharged heat (i.e. lower efficiency) as revealed in Fig. 9. This difference in LCOS pinpoints the outperformance of the tank though its higher specific investment cost for the construction. Furthermore, it can be said that tank's outperformance is also attributed to lower SA/V values compared to that of the corresponding shallow pit. Consequently, the hybrid TES emerges as a feasible promising compromise between both other options. The hybrid is capable to encompass the advantages of both geometries (i.e. high efficiency of tanks and low specific costs of pits).

To examine the impact of TES geometry on stratification quality, Fig. 12 compares the TES temperature at specific location for the considered TES shapes with a volume of 100,000 m^3. The locations are: TES top, height at which the TES volume is halved (i.e. corresponding to 50,000 m^3) and TES bottom. Fig. 12 exemplifies that a tank with (H/d = 1) arises as the best option compared to other TES geometries since the temperatures (top, mid and bottom) remain at higher levels. Compared to the shallow pit, the tank particularly is capable to maintain high temperature over the standby phase. In other words, the tank suffers from less impact of buoyancy-induced mixing and, therefore, better stratification quality. The hybrid, on the other hand, arises as a geometrical compromise between both other options. Moreover, Fig. 12 shows 4 operation phases for the TES that: charging, standby, discharging and idle, which correspond to A, B, C and D, respectively.

Fig. 13 shows the development of stratification number and stratification efficiency for a 100,000 m^3 TES. In this context, four TES operative phases are clearly recognized that are: charging, standby, discharging and idle. The results obviously exhibit the outperformance of the tank shape compared to other counterparts. The shallow pit, on the other hand, has the poorest quality of stratification as its quality drastically drops down to 60 % throughout charging and discharging phases. The hybrid TES, on its part, is capable to maintain a moderate quality as it shows better stratification compared to that of the shallow pit.

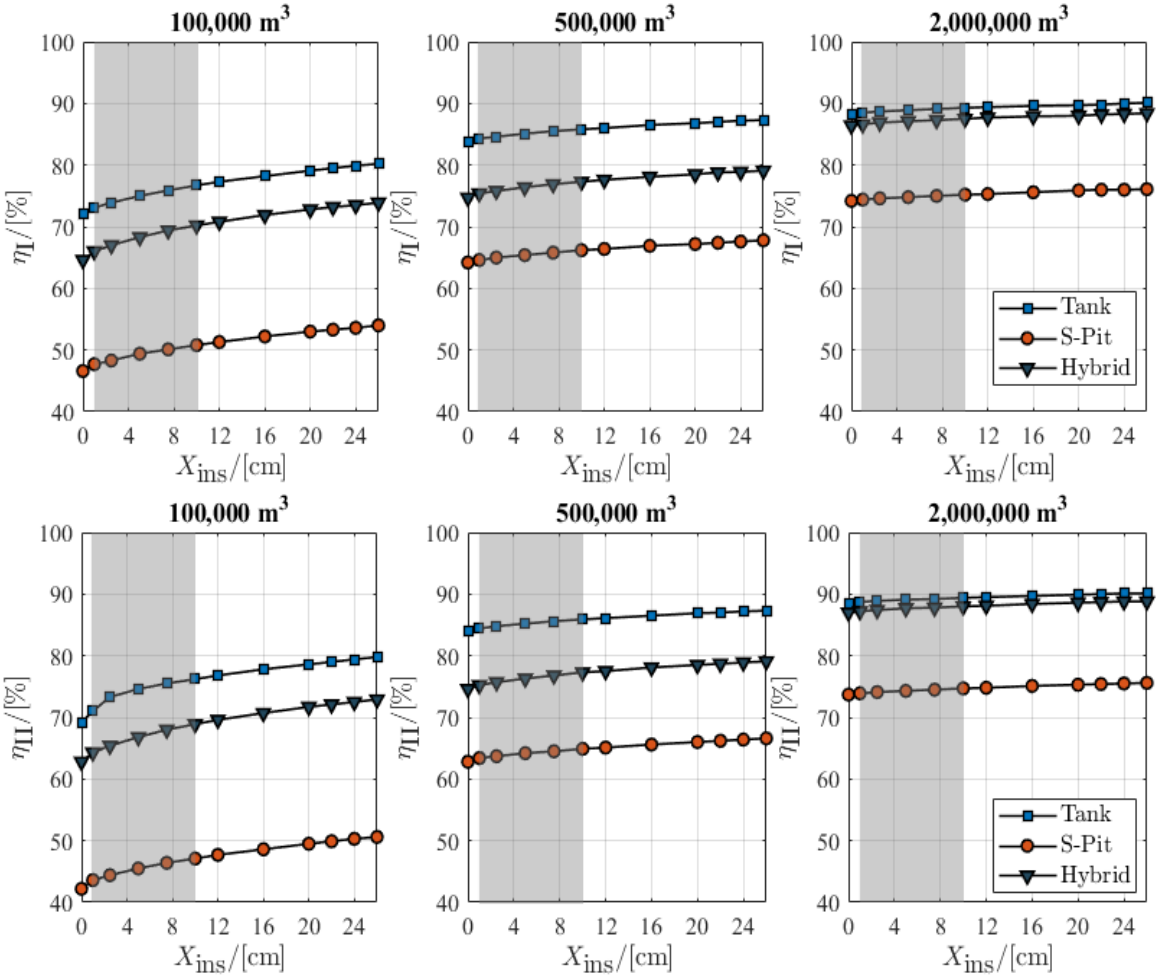

Fig. 9: Energy efficiency for 3 TES geometries (tank, shallow pit and hybrid) with a volume of 100,000 m^3. (Note: the grey-shaded region represents only a theoretical range as such small insulation layers are unpractical).

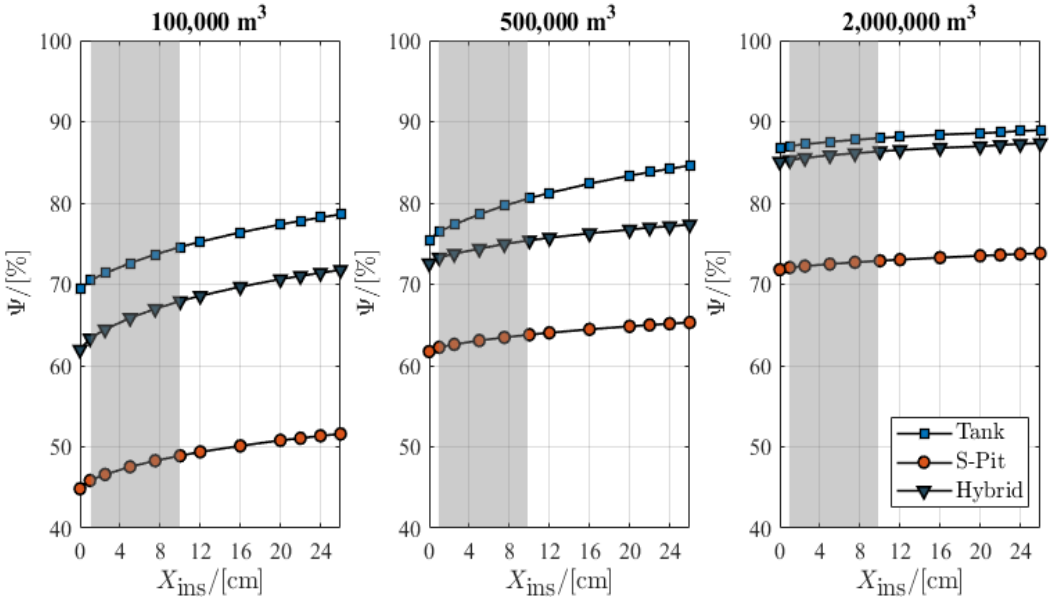

Fig. 10: Exergy efficiency for 3 TES geometries (tank, shallow pit and hybrid) with a volume of 100,000 m^3. (Note: the grey-shaded region represents only a theoretical range as such small insulation layers are unpractical).

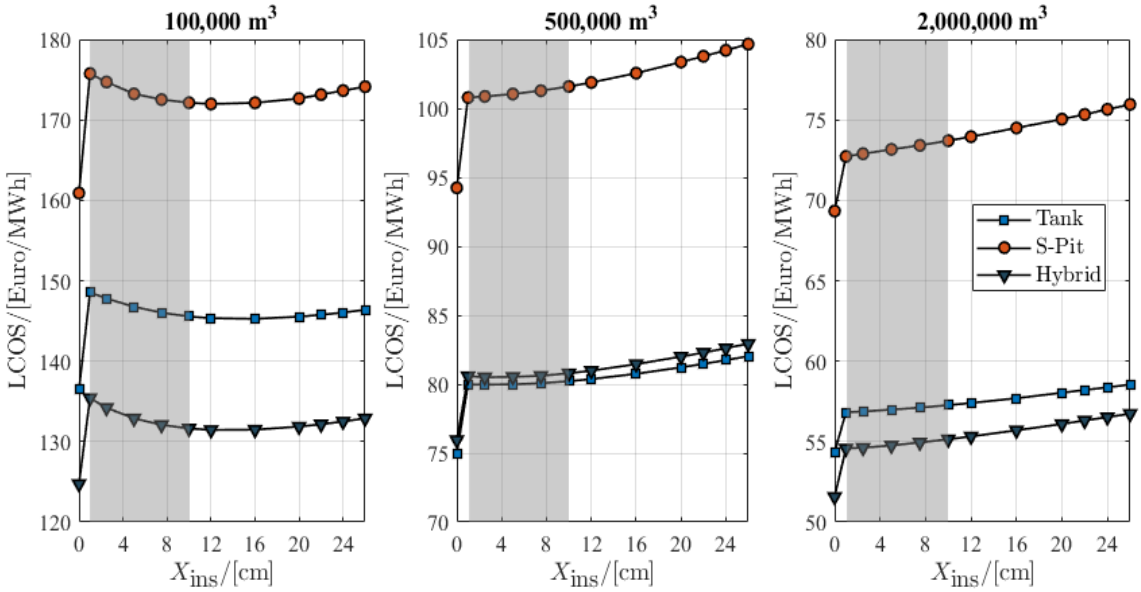

Fig. 11: Comparison of the levelized cost of stored heat over insulation thickness for three TES geometries. (Note: the grey-shaded region represents only a theoretical range as such small insulation layers are unpractical).

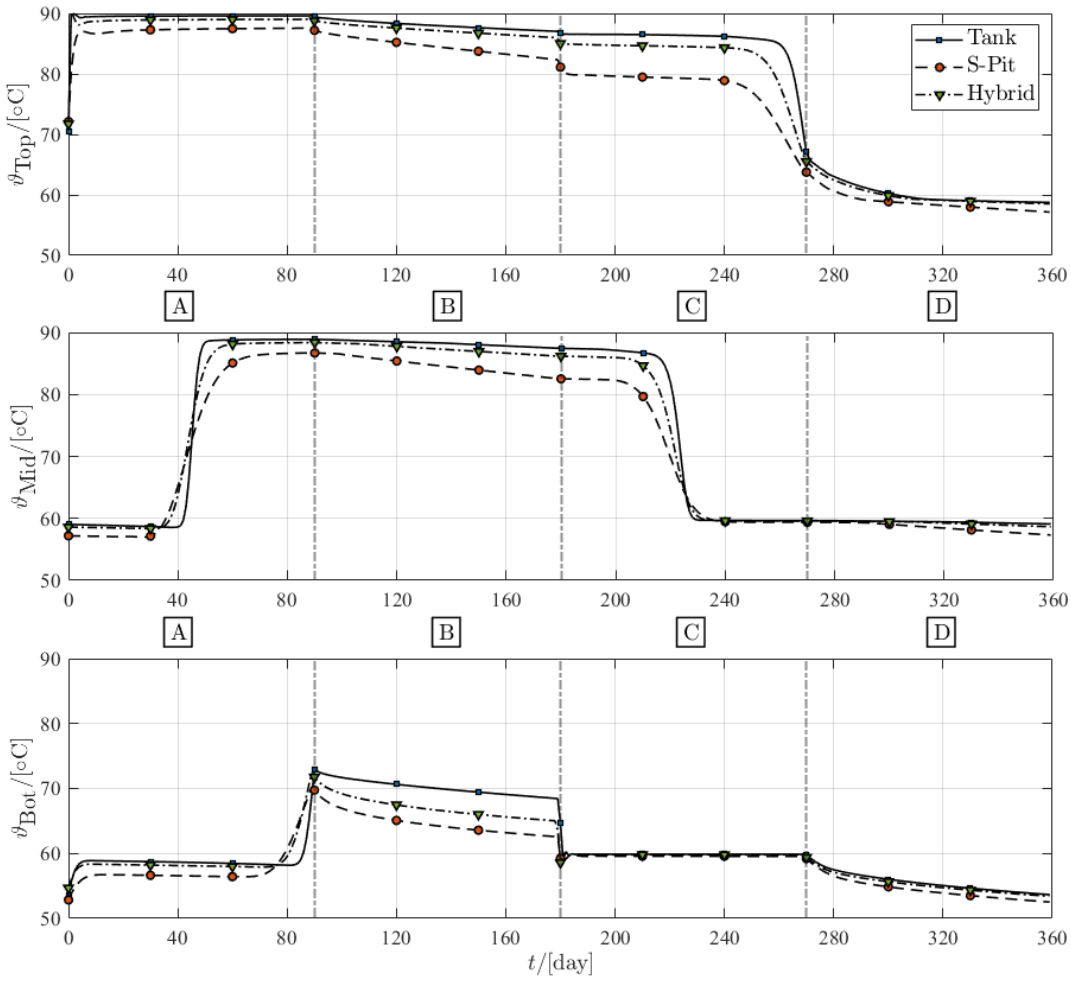

Fig. 12: Evolution of TES temperature at three locations (top, middle and bottom) over the 5th year for a 100,000 m^3 TES with U_{top} = 0.1 W/(m^2.K) and insulation thickness of 26 cm for the TES bottom and sidewalls. Mid refers to the location at which the TES has its half volume (i.e. 50,000 m^3).

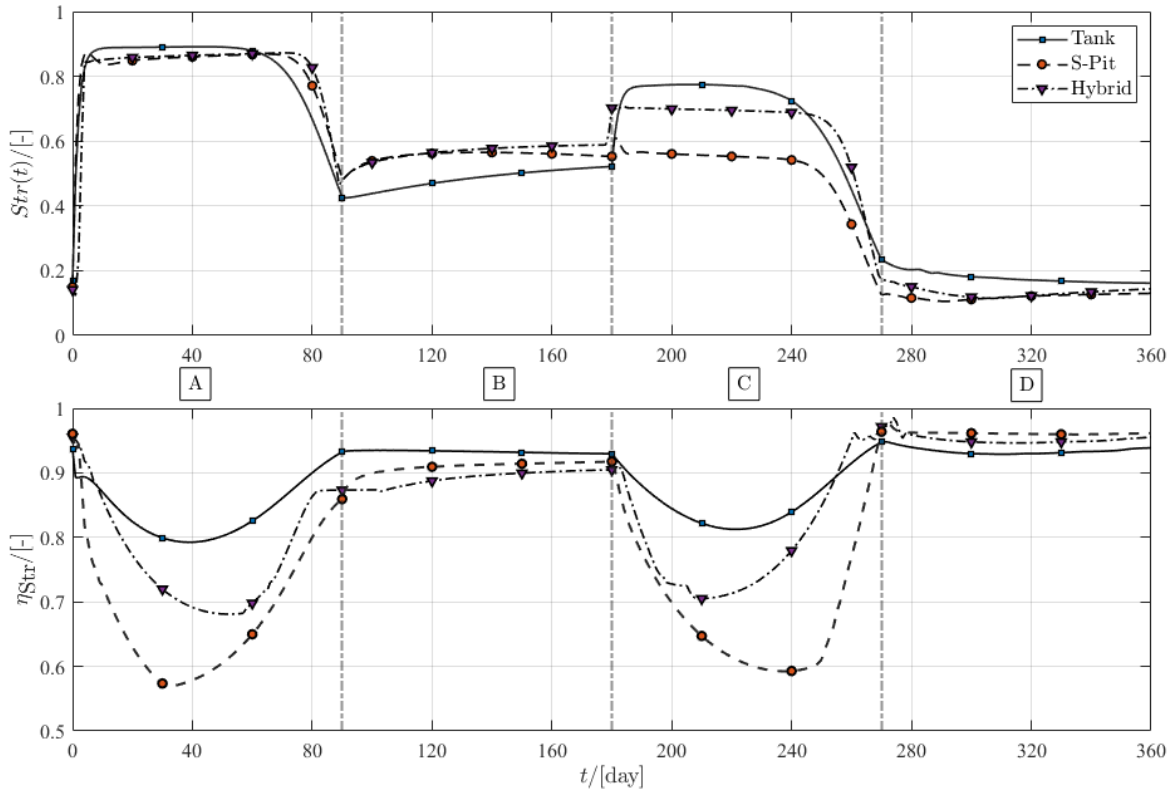

Fig. 13: Stratification number and stratification efficiency development over the 5th year for a 100,000 m^3 TES with U_{top} = 0.1 W/(m^2.K) and insulation thickness of 26 cm for the TES bottom and sidewalls.

C. Impact of DH characteristics

Having seen the impact of TES geometry on the economic considerations and technical performance, it becomes crucial to inspect another parameter. Herein, the parameter is an operative one as it is defined by the DH system into which the TES is integrated. In this context, this section considers a tank with two TES volumes. Fig. 14 compares two configurations, one is HT-DH and the other is LT-DH under same boundary conditions (e.g. ground thermal properties).

The LT-DH does not only lead to a reduction in the thermal losses, but it also brings a reduction in LCOS due to the increase in the discharged amount of heat out of TES. Besides, the installation of TES in LT-DH systems means operative temperature below 90°C and, thus, stainless-steel liners are not required. Instead, polymer liners are sufficient as their resistance to temperatures rises up to 85°C. Accordingly, an LCOS drop of around 25 €/MWh can be attained when a transition from a HT-DH to LT-DH is envisioned. The LCOS difference to approx. 10 €/MWh if the TES volume increases up to 2,000,000 m^3. In this context, the increase of TES volume leads to a reduction in the TES specific investment cost and, thus, the liner cost has less contribution to the total specific investment cost compared to a TES volume of 100,000 m^3. Besides, the performance difference between tanks installed in LT-DH and HT-DH decreases when larger volumes are achieved as demonstrated by Fig. 15. Moreover, it is essential to mention that the temperature difference in LT-TES systems is 50 K, whilst HT-TES has a difference of 30 K and, thus, an impact on the performance and storage capacity. Subsequently, this also has an impact on the levelized cost of stored heat.

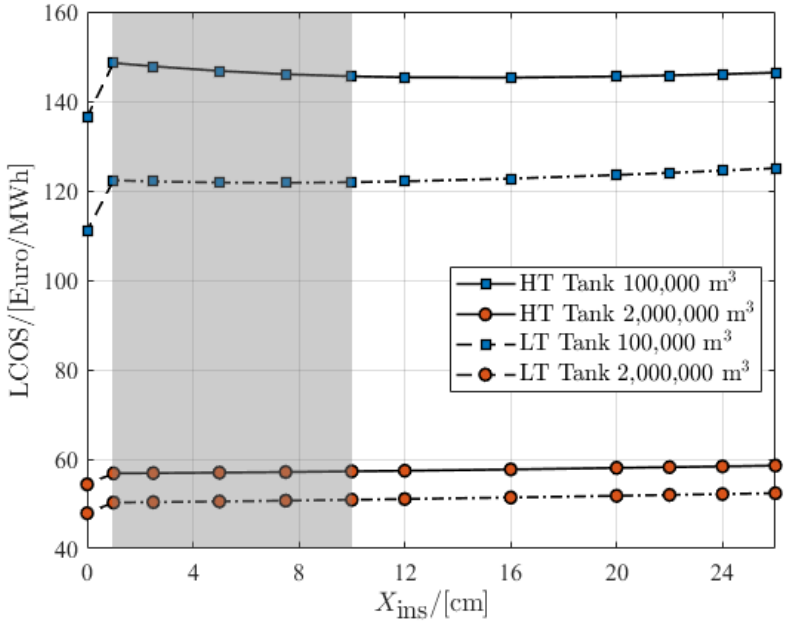

Fig. 14: Evolution of tank LCOS and performance over different insulation thicknesses in low- and high-temperature DH systems for two TES volumes; 100,000 m^3 and 2,000,000 m^3. (Note: the grey-shaded region represents only a theoretical range as such small insulation layers are unpractical).

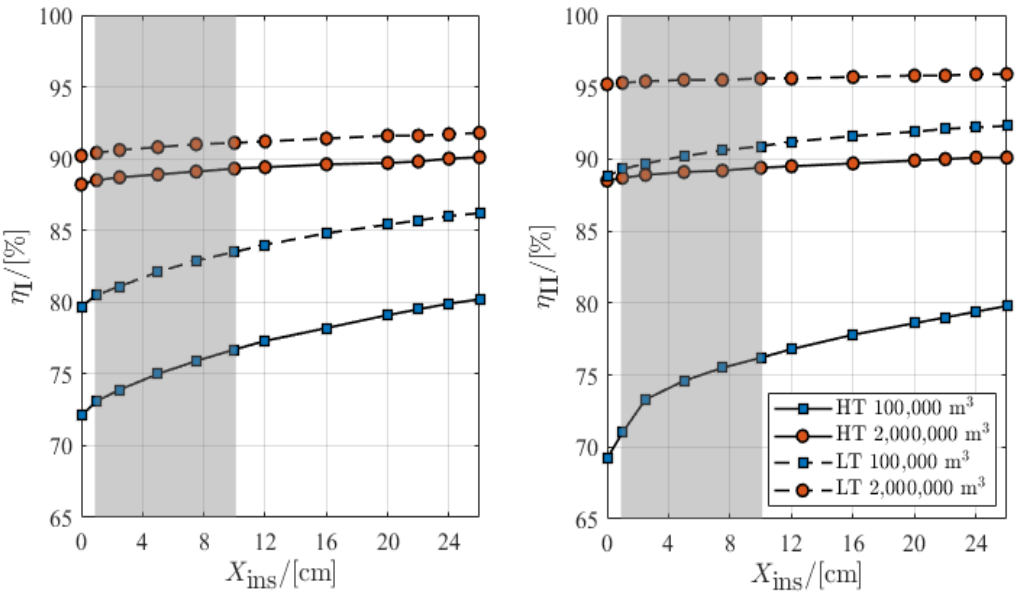

(a) TES energy efficiency (b) TES energy capacity efficiency

Fig. 15: Evolution of TES performance over different insulation thicknesses in low- and high-temperature DH systems for two TES volumes; 100,000 m^3 and 2,000,000 m^3. (Note: the grey-shaded region represents only a theoretical range as such small insulation layers are unpractical).

D. Impact of insulation

In the aforementioned sections, the investigated TES types were insulated in a uniform manner as insulation thickness was constant (i.e. homogenous distribution). Yet, these systems are stratified and, accordingly, hot water gathers at the top, while cold water favorably finds its place at the bottom. In this regard, Fig. 16 shows two possible options for insulation distribution in the TES envelope. Option (a) illustrates the TES insulation with a homogenous thickness, whilst (b) proposes a different insulation distribution with consideration of economic feasibility and technical performance to maintain stratification at a better status and costs as minimum.

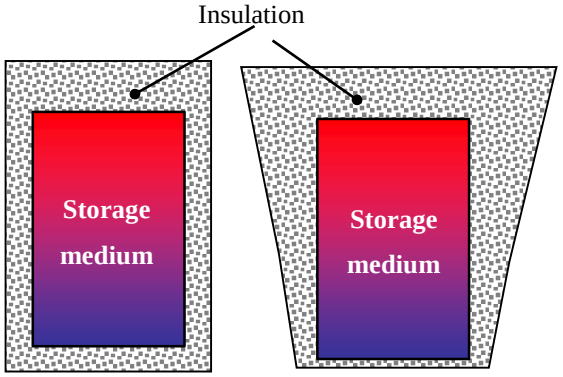

Fig. 16: Illustration of homogenous and inhomogeneous insulation distribution.

To compare both options, the general characteristics are as follows:

- Tank with a height of 50 m,
- 3 volumes of [100,000 500,000 2,000,000] m^3,
- Top insulation thickness is 53 cm, which is equivalent U_{top} = 0.1 W/(m^2.K),
- Insulation thermal conductivity, λ_{ins} = 0.08 W/(m.K).

TABLE VII reports the comparison results in terms of TES energy efficiency between both insulation cases for the different TES volumes considered. This comparison includes both DH systems for operation boundary conditions. It is revealed that the adaptation to inhomogeneous insulation (option (b)) results in a slight improvement (~ 3 %) in the TES energy efficiency for 100,000 m^3. Whereas it decreases to (< 1 %) if the TES volume increases up to 2,000,000 m^3.

TABLE VII. COMPARISON OF ENERGY EFFICIENCY FOR THE TWO INSULATION CASES SHOWN IN FIG. 16.

	HT η_I [%]		**LT** η_I [%]	
	(a)	**(b)**	**(a)**	**(b)**
100,000 [m^3]	80%	83%	86%	88%
500,000 [m^3]	88%	90%	92%	93%
2,000,000 [m^3]	90%	91%	93%	94%

TABLE VIII reports a comparison of LCOS between constantly insulated and inhomogeneous-insulated tanks. The comparison includes both system operation conditions (HT and LT). Therein, the installation of inhomogeneous distribution yields a reduction of 5 €/MWh for tanks with 100,000 m^3 installed in HT-DH system. However, this reduction decreases down to 1 €/MWh as the tank volume increases up to 2,000,000 m^3. The table also reports a similar trend for LT-DH systems but with lower values.

TABLE VIII. COMPARISON OF LEVELIZED COST OF STORED HEAT (LCOS) IN €/MWH FOR THE TWO INSULATION CASES SHOWN IN FIG. 16.

	HT LCOS (€/MWh)		**LT** LCOS (€/MWh)	
	(a)	**(b)**	**(a)**	**(b)**
100,000 [m^3]	146	141	135.5	134
500,000 [m^3]	81	79	70.5	70
2,000,000 [m^3]	56	57	52	52

V. CONCLUSIONS

Due to the current challenges with climate change and global warming, a transition to sustainable energy sources must be in action in order to satisfy the satiable, increasing society's need for energy. To systematically and successfully accomplishment of this transition, innovative technologies must undergo a research and development phase in order to commercialize such technologies and systems and implement them in a broader context. Amongst others, large-scale seasonal thermal energy storage (TES) arises as a central element for this transition in the heating and cooling sector.

Due to the large volume of such storages, the complexity in planning and construction of these stores drastically increases leading to a difficulty in decision—making process. Thus, this work discussed the players affecting the planning and construction of such stores. Further, the work reviewed recent literature in this context highlighting their outcomes and shortcomings.

The work investigated the influence of insulation thickness and TES geometry on the specific investment cost. The findings showed that the proposed hybrid outperformed its counterparts due to the lowest specific investment cost with major contribution of insulation. Not only economic consideration proved the feasibility of such a type, but also the technical evaluation emphasized its importance as competitor to the typical TES geometries. As a result, the work proposed the levelized cost of stored heat as a techno-economic metric and, subsequently, the results depicted the effectiveness of a hybrid TES.

The further examined the impact of the operation conditions on the TES energy efficiency and LCOS. In this regard, the DH temperature was the main central element under investigation. The results depicted that a transition to lower operation temperatures resulted in improvement in efficiency compared to its counterpart

BauSIM 2020 (Virtual): 8th Conference of IBPSA Germany and Austria, Graz, Austria, 2020.

in high temperature systems. As a result, LCOS also indicated lower values.

Moreover, it is important to stress out that earlier studies showed the economic feasibility of the shallow pit compared to tank. However, the chosen dimensions in this work differed from those reported earlier in order to highlight the role of shallow pit dimensions on the specific investment cost.

ACKNOWLEDGMENT

This project is financed by the Austrian "Klima- und Energiefonds" and performed in the frame of the program "Energieforschung". It is part of the Austrian flagship research project "Giga-Scale Thermal Energy Storage for Renewable Districts" (giga_TES, Project Nr.: 860949). Therefore, the authors wish to acknowledge the financial support for this work.

NOMENCLATURE

Symbol	Description	Unit
A	Cross-section area	m^2
ANF	Annuity factor	%
C	Cost	€
c	Specific cost	€/m^3
c_p	Specific heat capacity	J/(kg.K)
dz	Incremental length	m
E	Energy content	J
EX	Exergy	MWh
H	Height	m
i	Representative segment	%
L	Lifetime	years
LCOS	Levelized cost of stored heat,	€/MWh
M_E	Moment of energy	J.m
n	Number of segments	-
Q	Heat	J
P	Perimeter	m
$\dot{Q}$	Heat flowrate	W
$\dot{q}$	Heat flowrate per unit length	W/m
r	Radius	m
SA	Surface area	m^2
$Str(t)$	Stratification number	-
T	Absolute temperature	K
t	Time	s
U	Overall heat transfer coefficient	W/(m^2.K)
V	Volume	m^3
$\dot{V}$	Volume flowrate	m^3/s
X	Thickness	m
z	Vertical coordinate inside TES	m
α	Slope	∘
Δ	Difference	-
η	Efficiency	%
ϑ	Temperature	°C
λ	Thermal conductivity	W/(m.K)
ρ	Density	kg/m^3
Ψ	Exergy efficiency	%

REFERENCES

[1] F. Ochs, A. Dahash, A. Tosatto and M. Bianchi Janetti, "Techno-economic planning and construction of cost-effective large-scale hot water thermal energy storage for Renewable District heating systems," Renewable Energy, vol. 150, pp. 1165-1177, 2019.

[2] T. Yang, W. Liu, G. Jan Kramer and Q. Sun, "Seasonal thermal energy storage: A techno-economic literature review," Renewable and Sustainable Energy Reviews, vol. 139, 2021.

[3] A. Mukherjee, L. Kumar, C. Subramaniam and S. K. Saha, "Performance evaluation of a seasonal residential space heating system based on thermochemical energy storage," Applied Thermal Engineering, vol. 194, 2021.

[4] W. Villasmil, M. Troxler, R. Hendry, P. Schuetz and J. Worlitschek, "Control strategies of solar heating systems coupled with seasonal thermal energy storage in self-sufficient buildings," Journal of Energy Storage, vol. 42, 2021.

[5] H. Mahon, D. O'Connor, D. Friedrich and B. Hughes, "A review of thermal energy storage technologies for seasonal loops," Energy, Vols. 239, Part C,, 2022..

[6] A. Dahash, F. Ochs, A. Tosatto and W. Streicher, "Toward Efficient Numerical Modeling and Analysis of Large-Scale Thermal Energy Storage for Renewable District Heating Systems," Applied Energy, vol. 279, 2020.

[7] M. Salvestroni, G. Pierucci, A. Pourreza, F. Fagioli, F. Taddei, M. Messeri and M. De Lucia, "Design of a solar district heating system with seasonal storage in Italy," Applied Thermal Engineering, vol. 197, 2021.

[8] A. Dahash, F. Ochs, M. Bianchi Janetti and W. Streicher, "Advances in seasonal thermal energy storage for solar district heating applications: A critical review on large-scale hot-water tank and pit thermal energy storage systems," Applied Energy, vol. 239, pp. 296-315, 2019.

[9] M. H. Abokersh, M. Vallès, L. F. Cabeza and D. Boer, "A framework for the optimal integration of solar assisted district heating in different urban sized communities: A robust machine learning approach incorporating global sensitivity analysis," Applied Energy, vol. 267, 2020.

[10] V. Panthalookaran, W. Heidemann and H. Müller-Steinhagen, "A new method of characterization for stratified thermal energy stores," Solar Energy, vol. 81, no. 8, pp. 1043-1054, 2007.

[11] M. Yang, Z. Wang, J. Yang, G. Yuan, W. Wang and W. Shi, "Thermo-economic analysis of solar heating plant with the seasonal thermal storage in Northern China," Solar Energy, vol. 232, 2022.

[12] D. Park, H.-M. Kim, D.-W. Ryu, B.-H. Choi, C. Sunwoo and K.-C. Han, "The effect of aspect ratio on the thermal stratification and heat loss in rock caverns for underground thermal energy storage," International Journal of Rock Mechanics and Mining Sciences, vol. 64, pp. 201-209, 2013.

[13] A. Dahash, F. Ochs, G. Giuliani and A. Tosatto, "Understanding the Interaction between Groundwater and Large-Scale Underground Hot-Water Tanks and Pits," Sustainable Cities and Society, vol. 71, 2021.

[14] A. Dahash, M. Bianchi Janetti and F. Ochs, "Detailed Axial Symmetrical Model of Large-Scale Underground Thermal Energy Storage," in Proceedings of the 2018 COMSOL Conference, Lausanne (Switzerland), 22-24 October 2018, 2018.

[15] A. Dahash, F. Ochs and A. Tosatto, "Techno-economic and exergy analysis of tank and pit thermal energy storage for renewables district heating systems," Renewable Energy, vol. 180, pp. 1358-1379, 2021.

[16] A. Dahash, F. Ochs and A. Tosatto, "Simulation-based design optimization of large-scale seasonal thermal energy storage in renewable-based district heating systems," in Proceedings of BauSIM 2020 (Virtual): 8th Conference of IBPSA Germany and Austria, Graz, Austria, 2020.